

# Easy Access to Metallic Copper Nanoparticles with High Activity and Stability for CO Oxidation

Renato V. Gonçalves,<sup>\*,†,‡</sup> Robert Wojcieszak,<sup>§,⊥</sup> Heberton Wender,<sup>||</sup> Carlos Sato B. Dias,<sup>#</sup> Lucas L. R. Vono,<sup>†</sup> Dario Eberhardt,<sup>□</sup> Sergio R. Teixeira,<sup>△</sup> and Liane M. Rossi<sup>\*,†</sup>

<sup>†</sup>Departamento de Química Fundamental, Instituto de Química, Universidade de São Paulo, Avenida Prof. Lineu Prestes 748, São Paulo 05508-000, São Paulo, Brazil

<sup>§</sup>Unité de Catalyse et Chimie du Solide, UCCS, UMR CNRS 8181, F-59655 Villeneuve d'Ascq, France

<sup>⊥</sup>Université Lille Nord de France, F-59000 Lille, France

<sup>||</sup>Instituto de Física, Universidade Federal do Mato Grosso do Sul, Avenida Costa e Silva s/n, Campo Grande 79070-900, Mato Grosso do Sul, Brazil

<sup>#</sup>Laboratório Nacional de Luz Síncrotron (LNLS), Rua Giuseppe Maximo Scolfaro 10.000, Campinas 13083-970, São Paulo Brazil

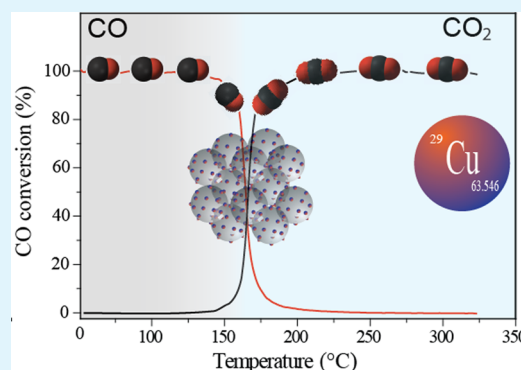
<sup>□</sup>Universidade de Caxias do Sul, Bento Gonçalves 95700-000, Rio Grande do Sul, Brazil

<sup>△</sup>Instituto de Física, Universidade Federal do Rio Grande do Sul, Avenida Bento Gonçalves 9500, Rio Grande do Sul, Brazil

## Supporting Information

**ABSTRACT:** Copper catalysts are very promising, affordable alternatives for noble metals in CO oxidation; however, the nature of the active species remains unclear and differs throughout previous reports. Here, we report the preparation of 8 nm copper nanoparticles (Cu NPs), with high metallic content, directly deposited onto the surface of silica nanopowders by magnetron sputtering deposition. The as-prepared Cu/SiO<sub>2</sub> contains 85% Cu<sup>0</sup> and 15% Cu<sup>2+</sup> and was enriched in the Cu<sup>0</sup> phase by H<sub>2</sub> soft pretreatment (96% Cu<sup>0</sup> and 4% Cu<sup>2+</sup>) or further oxidized after treatment with O<sub>2</sub> (33% Cu<sup>0</sup> and 67% Cu<sup>2+</sup>). These catalysts were studied in the catalytic oxidation of CO under dry and humid conditions. Higher activity was observed for the sample previously reduced with H<sub>2</sub>, suggesting that the presence of Cu-metal species enhances CO oxidation performance. Inversely, a poorer performance was observed for the sample previously oxidized with O<sub>2</sub>. The presence of water vapor caused only a small increase in the temperature require for the reaction to reach 100% conversion. Under dry conditions, the Cu NP catalyst was able to maintain full conversion for up to 45 h at 350 °C, but it deactivated with time on stream in the presence of water vapor.

**KEYWORDS:** magnetron sputtering deposition, copper nanoparticles, catalysis, carbon monoxide, CO oxidation



## INTRODUCTION

Problems associated with the exhaust emissions (NO<sub>x</sub>, CO, CO<sub>2</sub>, SO<sub>2</sub>, and hydrocarbons) from fossil fuels used in vehicles have attracted much attention because of their strong environmental impact, especially in urban areas where they are seriously impacting human health.<sup>1</sup> Among the various types of catalytic converters developed in the 1970s, the noble metals (Pt, Pd, Rh) are well-known to have a high activity for abatement of CO in exhaust emissions.<sup>2,3</sup> Two serious disadvantages of this kind of catalyst are their very high cost and their limited availability.<sup>3</sup> Over the past several decades, the development of new catalytic nanomaterials for CO oxidation based on transition metals oxides have attracted much interest.<sup>4,5</sup> Among them, increasing attention has been devoted to copper because of its abundance, low cost, and unique physical and chemical properties.

In the last 30 years, Cu-based materials with bulk, nano, and micro dimensions have attracted interest for catalytic CO oxidation.<sup>6–9</sup> However, both the Cu(I) and Cu(II) oxide species have been suggested as the most active sites for CO oxidation at relatively low temperatures.<sup>6,10</sup> White et al. prepared Cu<sub>2</sub>O nanoparticles via thermal decomposition reaction, which exhibited 99.5% conversion of CO to CO<sub>2</sub> at temperatures lower than 250 °C.<sup>10</sup> Wu et al. prepared partially oxidized copper nanoparticles supported on titania (Cu–Cu<sub>2</sub>O/TiO<sub>2</sub>) using a photodeposition method, which exhibited remarkably high activity and good stability for CO oxidation.<sup>11</sup> Huang et al. prepared CuO nanoparticles supported on titania (CuO/TiO<sub>2</sub>) using a deposition–precipitation method, which

Received: January 6, 2015

Accepted: March 27, 2015

Published: March 27, 2015

was also found to be active for CO oxidation.<sup>12</sup> Huang and Tsai studied CO oxidation in Cu, Cu<sub>2</sub>O, and CuO.<sup>7</sup> They concluded that Cu<sub>2</sub>O exhibits higher activities for CO oxidation than the other two copper species. Conversely, Wang et al. showed that very active copper-ceria catalysts contain Cu(II) as the sole active state present in O<sub>2</sub>-pretreated catalysts and, in the case of H<sub>2</sub>-pretreated sample, mixed Cu(II)/Cu(I) phases were present, with Cu(II) being the dominant state.<sup>13</sup> Thus, the question of which states are the true active sites still remains unanswered either because there is more than one active species or the species are not being properly identified by the techniques used in the catalyst characterization. Moreover, in all of these examples, the synthetic procedures varied; consequently, different species may have been adsorbed on the surface of the NPs. In some cases, a proper characterization of surface composition was not provided. The ideal methodology should result in metallic catalyst surfaces that are “as clean as possible”.

Recently, we have demonstrated that in addition to thin films, the magnetron sputtering deposition method is emerging as one of the most important and powerful forms of technology used to produce metal NPs in liquids<sup>14–17</sup> and powder support.<sup>18–20</sup> Because no stabilizing and reducing agents are required, the NP surfaces are free of contaminants. The method is promising for preparing metallic and/or metallic oxide NPs on the surface of a powder support. The sputtering deposition method involves ejecting atoms and/or atomic clusters from highly pure targets (99.99%) onto a substrate. The growth mechanism of thin film through sputtering has been extensively studied and it involves atoms/clusters nucleation, island growth, impingement and coalescence of the islands.<sup>21</sup> For the case in which NPs are sputtered onto liquids, the mechanism is not well understood and it seems to depend on several parameters such as liquid surface composition, surface tension, viscosity, surface coordination ability, discharge voltage and current, working pressure and distance, and the gas used for the process.<sup>14</sup> However, the mechanism for sputtered NPs onto powders is not yet known. It is expected to be strongly affected by the interaction between the substrate surface and the incoming sputtered atoms.<sup>22</sup>

In this present study, Cu NPs were directly deposited onto the surface of silica nanopowders using magnetron sputtering deposition. The sputtering sample holder was especially adapted for the deposition of metal NPs onto powder supports by using a mechanical agitation inside the vacuum chamber. Different NP compositions can be obtained by properly choosing the sputtering target. The catalytic properties of the Cu NPs/SiO<sub>2</sub> prepared by magnetron sputtering were, for the first time, investigated in the CO oxidation reaction.

## EXPERIMENTAL SECTION

**General Considerations.** All the solvents and reagents were of analytical grade and were used as received. Copper sputtering target (2 in., 99.99%) was purchased from Goodfellow Corporation (Coraopolis, PA, USA); tetraethyl orthosilicate (TEOS, 99.99%) and ethanol (99.99%) were purchased from Aldrich (St. Louis, MO, USA); and ammonium hydroxide (NH<sub>4</sub>OH) was purchased from Vetec Química (Brazil).

**Preparation of the Silica Nanospheres.** Silica nanospheres were prepared by a modification of the Stöber method.<sup>23</sup> Tetraethyl orthosilicate (1.3 mL) was premixed with ethanol (3.7 mL) and then added to a solution containing ammonium hydroxide (3.0 mL, 29% aqueous solution), water (3 mL) and ethanol (19 mL). After 1 h under stirring at room temperature, the SiO<sub>2</sub> nanospheres were separated by

centrifugation (7000 rpm, 20 min) and washed with ethanol (3×) and distilled water (1×). The obtained white powder was calcined in air for 2 h at 500 °C in order to remove any organic residue.

**Preparation of the Cu NPs.** Cu nanoparticles (Cu NPs) were directly deposited onto SiO<sub>2</sub> powders using a sputtering deposition system (Intercovamex-H5) with a specially designed mechanical resonant agitator placed inside the vacuum chamber, as previously reported.<sup>18,19</sup> This permits the SiO<sub>2</sub> powders to vibrate during Cu sputtering deposition in order to be homogeneously covered by the sputtered NPs. For the sputtering deposition, 100 mg of SiO<sub>2</sub> powder was placed into a glass support connected to the mechanical resonant agitator. Before sputtering, the vacuum chamber was pumped down  $2 \times 10^{-7}$  mbar for 24 h. In each experiment, sputtering was performed using the following conditions: 150 W,  $2 \times 10^{-3}$  mbar of working pressure, deposition time of 10 min, and a target-to-substrate distance of 5.0 cm. A vibration frequency of 50 Hz was maintained by a sinusoidal wave generation supplied during deposition. The deposited Cu mass was quantified using flame atomic absorption spectroscopy (FAAS).

**Microscopy Analysis.** The morphology of the prepared SiO<sub>2</sub> supports was investigated with an FEI Inspect F50 field-emission scanning electron microscope (FESEM), operated at 10 kV and 30 kV with a secondary electron detector. A high-resolution transmission electron microscope (HRTEM, model JEOL JEM 3010) operated at 300 kV was used to investigate both the morphologic and crystalline features of the Cu NPs. The samples were prepared by dispersing the Cu/SiO<sub>2</sub> powder in ethanol at room temperature and then depositing them onto a 400 mesh carbon-coated Cu grid. The histograms of the nanoparticle size distribution, assuming a spherical shape (in the case of SiO<sub>2</sub>) were obtained from measurements of more than 200 particles found in arbitrarily chosen regions of the grid. The histograms of the Cu-based NPs were fitted considering a log-normal distribution.

**X-ray Diffraction (XRD).** The XRD pattern of the samples was recorded with a Rigaku Miniflex diffractometer with Cu K $\alpha$  radiation ( $\lambda = 1.54 \text{ \AA}$ ) at  $2\theta = 25\text{--}90^\circ$  with a  $0.02^\circ$  step size. Rietveld profile refinement was performed with FullProf software.<sup>24</sup>

**Flame Atomic Absorption Spectroscopy (FAAS).** FAAS analysis to determine the concentration of Cu on Cu/SiO<sub>2</sub> was performed using a Shimadzu AA-6300 Atomic Absorption Spectrophotometer. The sample was digested in aqua regia (HNO<sub>3</sub>/HCl 1:3) before analysis. Initially, 10 mg of Cu/SiO<sub>2</sub> was added to a beaker with 5.0 mL of aqua regia solution and maintained at 110 °C for 3 h. After complete digestion, 5 mL of distilled water was added and the digestive solution was centrifuged at 7000 rpm (20 min) for complete separation of the remaining SiO<sub>2</sub> support. The volume of the supernatant was adjusted up to 10 mL for analysis. The spectrophotometer was calibrated with standard copper(II) solutions (0.5, 1.0, and 2.0 ppm) using distilled water as a blank.

**X-ray Absorption near-Edge Structure (XANES) Study.** XANES experiments were performed at the Cu K-edge (8979 eV) in the XAFS1 beamline at the Brazilian Synchrotron Light Laboratory (LNLS) (proposal XAFS1–15295). The spectra were collected in situ (during H<sub>2</sub> treatment) at different temperatures ranging from room temperature up to 500 °C, by using a channel-cut Si (111) crystal monochromator and three ionization chambers to detect incident and transmitted photon fluxes. During data collection, the XANES spectrum of a Cu foil was simultaneously measured and the energy calibrated by aligning the respective absorption edges. The data edge-step normalization was performed after a linear pre-edge subtraction and the regression of a quadratic polynomial beyond the edge, using ATHENA software.<sup>25</sup> The Cu and CuO spectra standards were collected in the same experimental condition and position of the sample in order to investigate the presence of CuO in the NPs; the data were further used for linear combination fittings for all temperature ranges.

**X-ray Photoelectron Spectroscopy (XPS).** XPS spectra were obtained using conventional equipment with a high-performance hemispheric analyzer (VG Escalab 220 XL spectrometer) with monochromatic Al K $\alpha$  ( $h\nu = 1486.6 \text{ eV}$ ) radiation as the excitation source. The operating pressure in the ultrahigh vacuum chamber

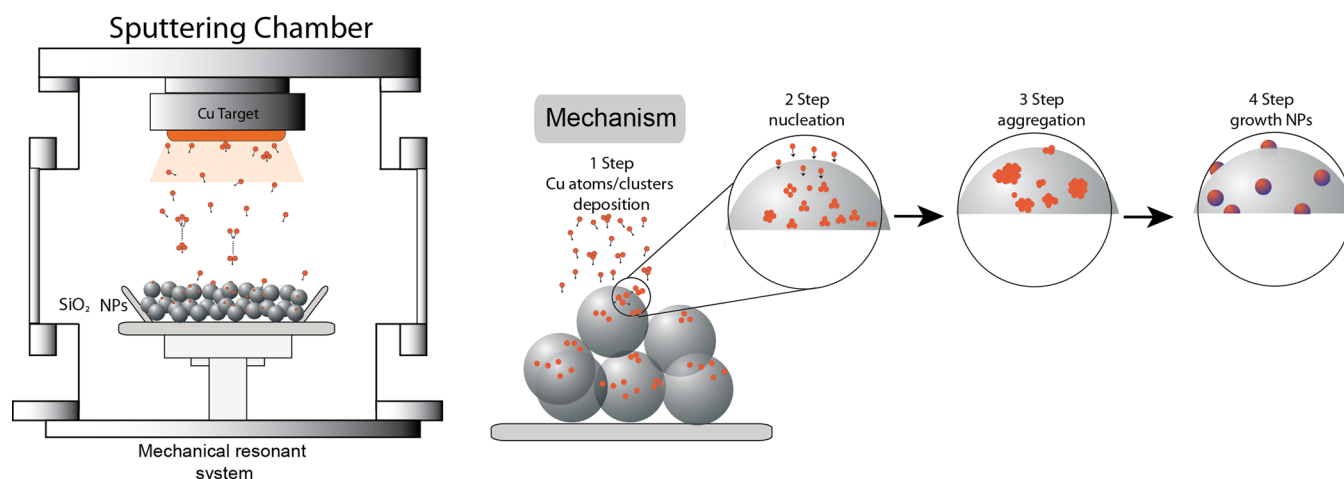


**Figure 1.** Schematic illustration of the process of copper nanoparticle formation by magnetron sputtering in a nanopowder support.

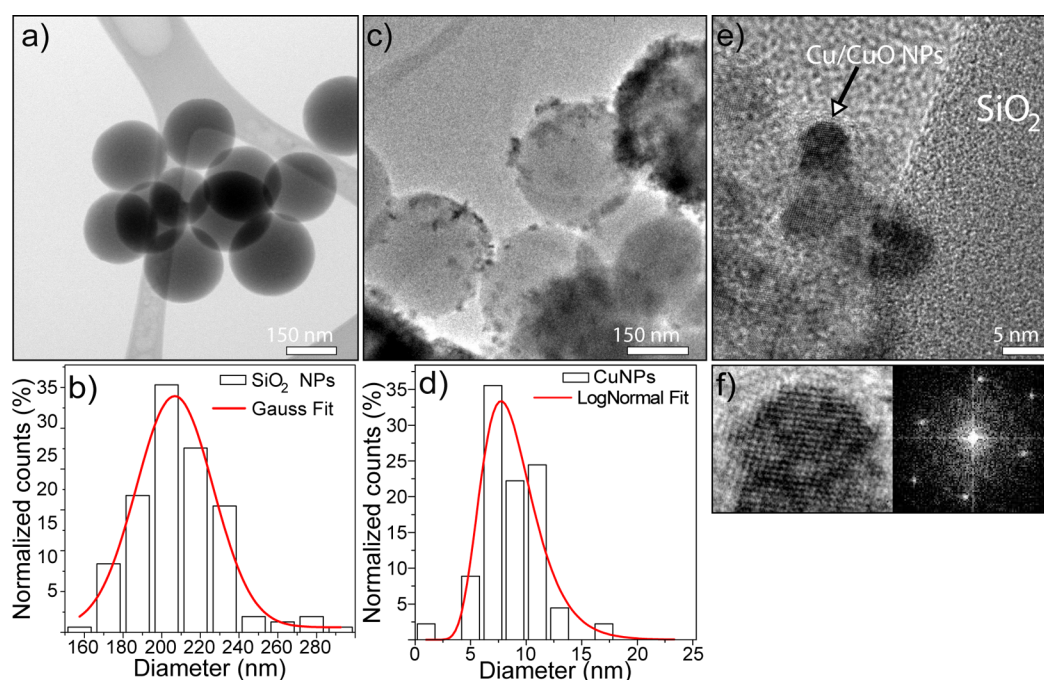


**Figure 2.** (a) STEM image of SiO<sub>2</sub> nanospheres; (b) size distribution histogram of SiO<sub>2</sub> nanospheres fitted to a Gaussian function; (c) TEM image of Cu NPs sputtering deposited onto the SiO<sub>2</sub> support; (d) size distribution histogram of Cu NPs fitted to a log-normal function; (e, f) HRTEM images of Cu NPs and the Fourier transform obtained using Gatan software.

(UHV) during the analysis was  $1 \times 10^{-9}$  Pa. Energy steps of 50 and 20 eV were used for the survey and single-element spectra, respectively. Peak decomposition was performed using a 70% Gaussian type curve and a 30% Lorentzian type curve, and a Tougaard nonlinear sigmoid-type baseline. The following peaks were used for the quantitative analysis: O 1s, C 1s, Cu 2p, Cu LVV, and Si 2p. Moreover, the Si 2p and C 1s peaks were also monitored to check for charge stability as a function of time. Molar fractions were calculated using peak areas normalized on the basis of the acquisition parameters after a background subtraction, and they were corrected with the experimental sensitivity and transmission factors provided by the manufacturer. The C-(C, H) component of the C 1s peak of adventitious carbon was fixed at 284.8 eV to set the binding energy scale, and the data treatment was performed using CasaXPS software (Casa Software Ltd, UK).

An XPS spectrometer coupled with a prepreparation chamber was used to determine the active species present on the surface of the materials after treatment under catalytic test conditions. Contrary to

the standard XPS analysis, this configuration permits in situ observation of active species. The samples were placed in the preparation chamber under reaction stream (H<sub>2</sub>, CO, O<sub>2</sub>) under controlled pressure and temperature; they were then transferred in situ into the analysis chamber of the spectrometer. The catalyst can be submitted to a reduction process with hydrogen (or an oxidation process with O<sub>2</sub>) inside of the XPS spectrometer, avoiding contact of the sample with air. The samples were treated with hydrogen or oxygen at 200 °C for 2 h. After that, the sample was cooled and the XPS analysis was performed as described above.

**Catalytic CO Oxidation.** The CO oxidation activity measurements were performed using 20 mg of Cu/SiO<sub>2</sub> powder placed in a quartz tube reactor (length, 20 mm; width, 5 mm). A continuous flow of the reactant mixture containing 1.75 vol % CO, 15 vol % O<sub>2</sub>, and Ar balance was passed through the reactor with a total flow rate of 100 mL min<sup>-1</sup>. The CO oxidation reaction under humid condition was conducted by passing the Ar stream through a thermostated saturator for adding water vapor to the carrier gas (1 and 5 vol %). The reaction

was performed on an Integrated Microreactor-MS system equipped with a CATLAB-PCS module and a QIC-20 MS module (Hiden Analytical, UK). The samples were used as-prepared or treated with H<sub>2</sub> (5 vol % and Ar balance) or O<sub>2</sub> (50 vol % and Ar balance) before the catalytic tests.

## RESULTS AND DISCUSSION

**Cu NPs Prepared by the Sputtering Deposition Method.** To allow the sputtering deposition of atoms/clusters on a powder support, we specifically developed a mechanical resonant system and placed it inside the sputtering chamber, as reported elsewhere.<sup>18,19</sup> A schematic representation of the mechanical resonant sputtering system and a suggested mechanism of Cu NPs formation on the surface of a SiO<sub>2</sub> nanopowder are shown in Figure 1. Initially, in the physical regime adopted for sputtering in our experiments, Cu atoms/clusters were ejected from the sputter target and deposited onto the surface of the SiO<sub>2</sub> nanopowders that were continuously being mechanically agitated. In terms of the growth mechanism, a discrete nucleation of atoms/clusters may occur on the surface of the SiO<sub>2</sub> support. The islands that have already formed can grow in size, thereby forming metallic nanoparticles similar to what is proposed for thin films. In contrast to the static flat substrates, herein the nucleation occurs at a spherical surface that is under continuous agitation. It strongly diminishes the kinetics of nucleation and growth because the atoms/clusters are deposited in different regions on the surface of the support, avoiding the growth of islands very close to each other and, consequently, the complete coverage of the support by a thin film.

The SiO<sub>2</sub> nanopowder used as support for the sputtering deposition of the Cu NPs catalyst was prepared by a modification of the Stöber method.<sup>23</sup> The morphology of the SiO<sub>2</sub> nanopowder was examined by TEM (Figure 2a). The sample contains spherical particles and Gaussian size distribution with a mean diameter of 207 ± 20 nm (Figure 2b), as also corroborated by SEM analysis (see the Supporting Information, Figure S1). The morphology and size of the sputtering deposited Cu NPs catalyst was examined by TEM (Figure 2c, e) and HRTEM (Figure 2f) images. The size distribution histogram presented in Figure 2d revealed spherical NPs with a log-normal size distribution and a mean diameter of 8.8 ± 2.7 nm. The interplanar distance, obtained by applying a fast Fourier transform (FFT) algorithm in the HRTEM image shown in Figure 1f (the zone of analysis is indicated by a white arrow in Figure 2e), suggested the presence of a mixture of Cu and CuO. The observed distances of 1.90, 2.27, 2.37, and 2.63 Å are in agreement with the (200) plane of metallic Cu (ICSD 00–004–0836) and with the (200), (111), and (002) planes of CuO (ICSD 00–044–0706), respectively. The Cu content in the sample was determined as 1.2 wt % by FAAS (10 min of sputtering deposition).

**XRD and XANES Studies.** The crystalline structure of the Cu NPs was analyzed by X-ray diffraction (XRD) in combination with Rietveld refinement, and the results are shown in Figure 3. As seen in Figure 3, the XRD patterns of the Cu NPs shortly after synthesis showed only the metallic phase of Cu (JPCDS file 4–836) with a cubic structure. The applied Rietveld refinements showed that the refined cell parameters are 4.0851 Å and the grain size of the Cu is about 8 nm with a preferred orientation in the (111) direction. The results obtained by XRD suggest the presence of the Cu(0) phase;

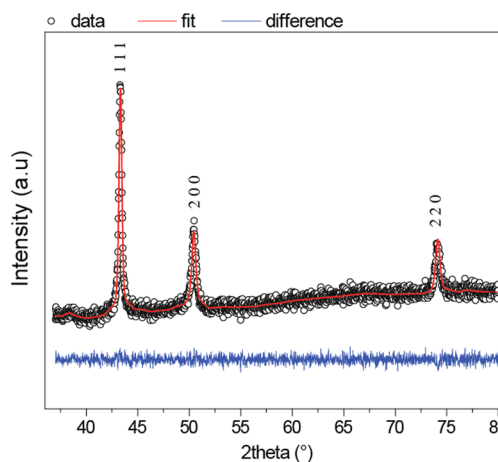


**Figure 3.** XRD pattern and Rietveld refinement of the Cu NPs sputter-deposited onto SiO<sub>2</sub>.

however, this does not exclude the presence of oxidized species on the crystallite surfaces.

Other techniques were applied to better describe the material obtained by magnetron sputtering. X-ray absorption near-edge structure (XANES) is one of the most powerful techniques used to obtain detailed electronic and structural information about the composition of materials. Herein, XANES measurements were used to characterize the Cu NPs soon after sputtering deposition and after H<sub>2</sub> and O<sub>2</sub> pretreatment (Figure 4). The percentage compositions of the copper species in the as-prepared samples and the samples after H<sub>2</sub> and O<sub>2</sub> pretreatments were quantified using a linear combination fitting of the XANES spectra. Figure 4a shows the XANES spectra of the as-prepared Cu NPs. The XANES spectrum indicates that the Cu NPs are predominantly metallic. Linear combination fittings of the XANES spectra using standard Cu<sup>0</sup> and Cu<sup>2+</sup> spectra revealed that the as-prepared Cu/SiO<sub>2</sub> nanocomposite had a mixture of 85% and 15% of Cu<sup>0</sup> and Cu<sup>2+</sup>, respectively (at 25 °C). Copper NPs tend to oxidize quickly when exposed to air, which explains the presence of the Cu<sup>2+</sup> detected by XANES. However, the Cu oxide phase can be reduced to Cu metal under H<sub>2</sub> treatment at 200 °C for 2 h (soft pretreatment). The linear combination of the XANES spectra of the sample after H<sub>2</sub> treatment showed a chemical composition of 96% and 4% of Cu<sup>0</sup> and Cu<sup>2+</sup>, respectively (Figure 4b). On the other hand, when the catalyst was pretreated under O<sub>2</sub> at 200 °C for 2 h (soft pretreatment), the Cu<sup>0</sup> phase is oxidized to Cu<sup>2+</sup> (CuO). Linear combination fittings of the XANES spectra revealed a mixture of 33 and 67% Cu<sup>0</sup> and Cu<sup>2+</sup>, respectively, after O<sub>2</sub> treatment (Figure 4c).

**XPS Studies.** An XPS study determines the chemical state of the species present on the catalyst surface. The results are given in Table 1 and Figure 5. XPS molar concentrations and Cu 2p binding energies for all the samples confirmed the presence of different copper species on the surface of the catalysts. The peak at the lowest binding energy, in the Cu 2p region, at about 932.2 eV of the H<sub>2</sub> pretreated samples, can be assigned either to Cu<sup>0</sup> or Cu<sup>+</sup> (Figure 5b). These Cu species are not easily distinguished from analysis of the Cu 2p region only.<sup>26</sup> However, analysis of the Cu<sub>LVV</sub> Auger peak can help distinguish them. The sample that was reduced with H<sub>2</sub> at 200 °C showed a sharp peak at about KE = 918 eV (see the Supporting Information, Figure S2), which should be assigned to the Cu<sup>0</sup> species.<sup>26</sup> In contrast, the as-prepared sample

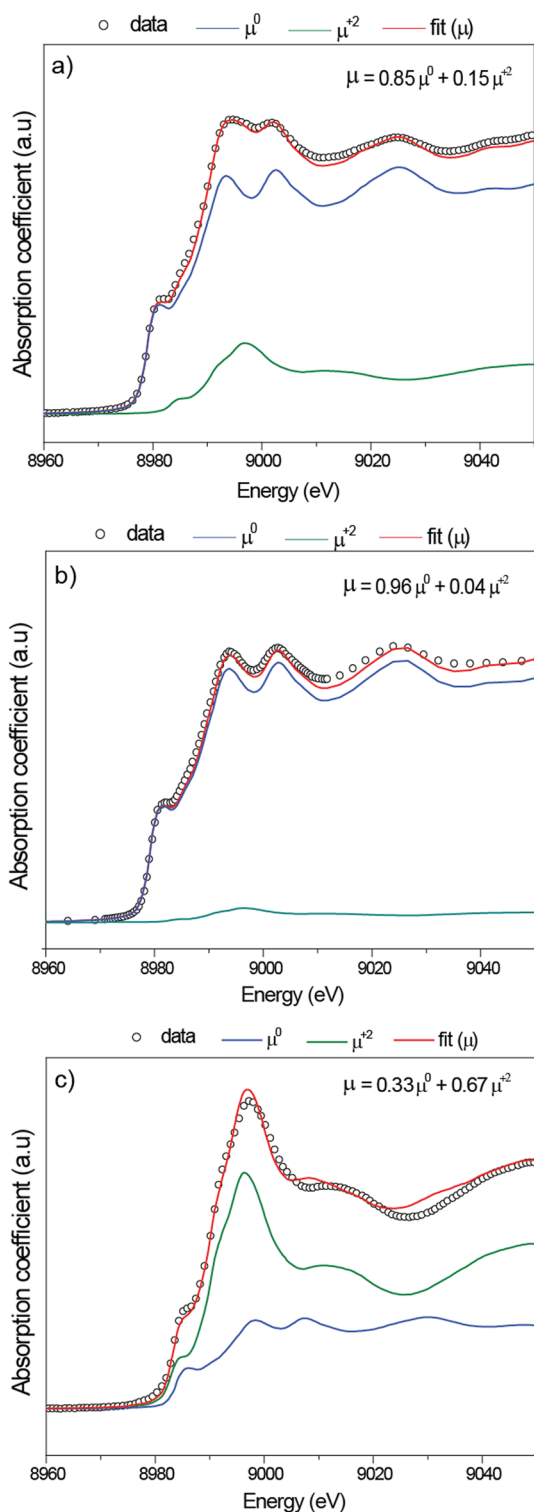


**Figure 4.** XANES spectra of the Cu NPs catalyst: (a) as-prepared catalyst, (b) after H<sub>2</sub> treatment (200 °C, 2 h), and (c) after O<sub>2</sub> treatment (200 °C, 2 h).

showed one broad peak at about 917 eV that originated from CuO.

In the case of the as-prepared sample, two additional broad peaks, at about BE = 934.2 and 943 eV, were observed and this confirmed the presence of the Cu<sup>2+</sup> phase (the 2p<sub>3/2</sub> contribution and the Cu<sup>2+</sup> satellite peak, respectively) (Figure 5a). As expected, higher Cu<sup>0</sup> content was found for the H<sub>2</sub>

**Table 1.** Chemical Composition and XPS Molar Ratios

catalyst	Cu (%)		O (%)	Si (%)	C (%)
	Cu <sup>0</sup>	Cu <sup>2+</sup>			
as-prepared	0.7	5.7	55.3	20.5	17.8
H <sub>2</sub> pretreated <sup>a</sup>	4.5	0.7	60.0	29.4	5.3
O <sub>2</sub> pretreated <sup>a</sup>		5.7	57.8	26.8	4.8
spent sample <sup>b</sup>		2.8	60.8	27.4	9.0

<sup>a</sup>Samples pretreated at 200 °C. <sup>b</sup>Catalyst after reaction.

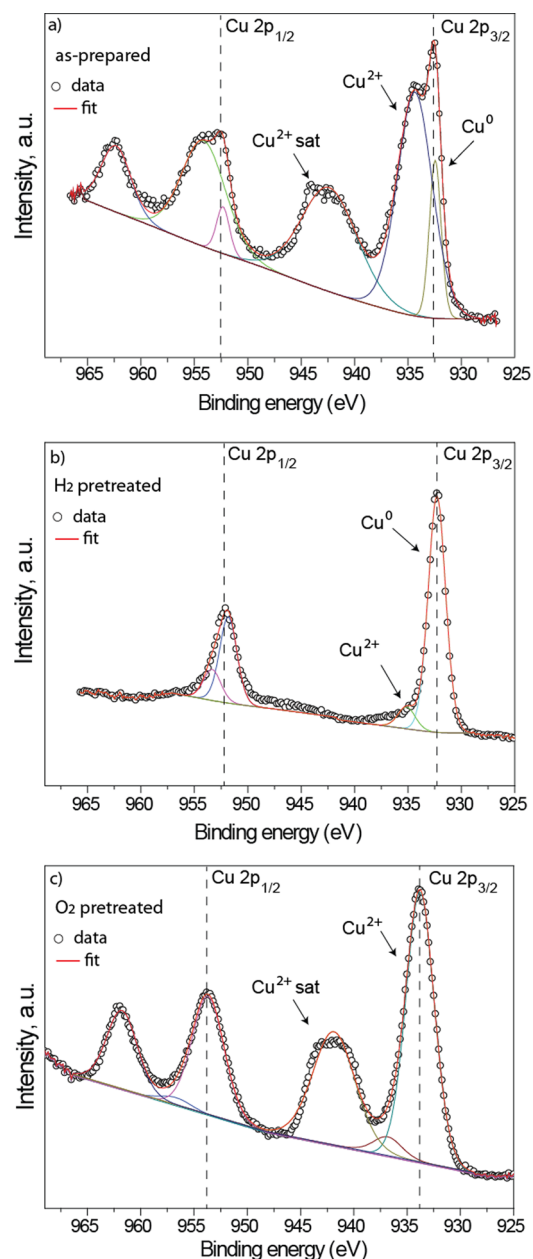


**Figure 5.** XPS spectra of the Cu 2p region for Cu/SiO<sub>2</sub>: (a) as-prepared catalyst, (b) after H<sub>2</sub> treatment (200 °C, 2 h), and (c) after O<sub>2</sub> treatment (200 °C, 2 h).

reduced sample (Figure 5b). The molar ratio confirmed that more than 86% of the copper atoms on the surface were Cu<sup>0</sup>. Only 11% of the surface atoms were Cu<sup>0</sup> in the case of the as-prepared sample. These results are in agreement with the results obtained by XANES and the TEM analysis. Indeed, the

XANES results showed that 15% of the Cu atoms were in the  $\text{Cu}^{2+}$  state. Those  $\text{Cu}^{2+}$  ions were localized essentially on the surface of the Cu NPs, as shown from the XPS analysis (89% of  $\text{Cu}^{2+}$ ). The  $\text{O}_2$  pretreated sample was completely oxidized and it contains only the  $\text{Cu}^{2+}$  phase (Figure 5c). The low carbon contamination that was observed for the spent sample (Table 1) confirmed that there is no carbon deposition on the catalyst after the catalytic cycle.

**CO Oxidation Activity.** The catalytic activity of the Cu/SiO<sub>2</sub> NP catalyst prepared by magnetron sputtering deposition was tested in the CO oxidation reaction and the results are shown in Figure 6 and summarized in Table 2. The SiO<sub>2</sub>

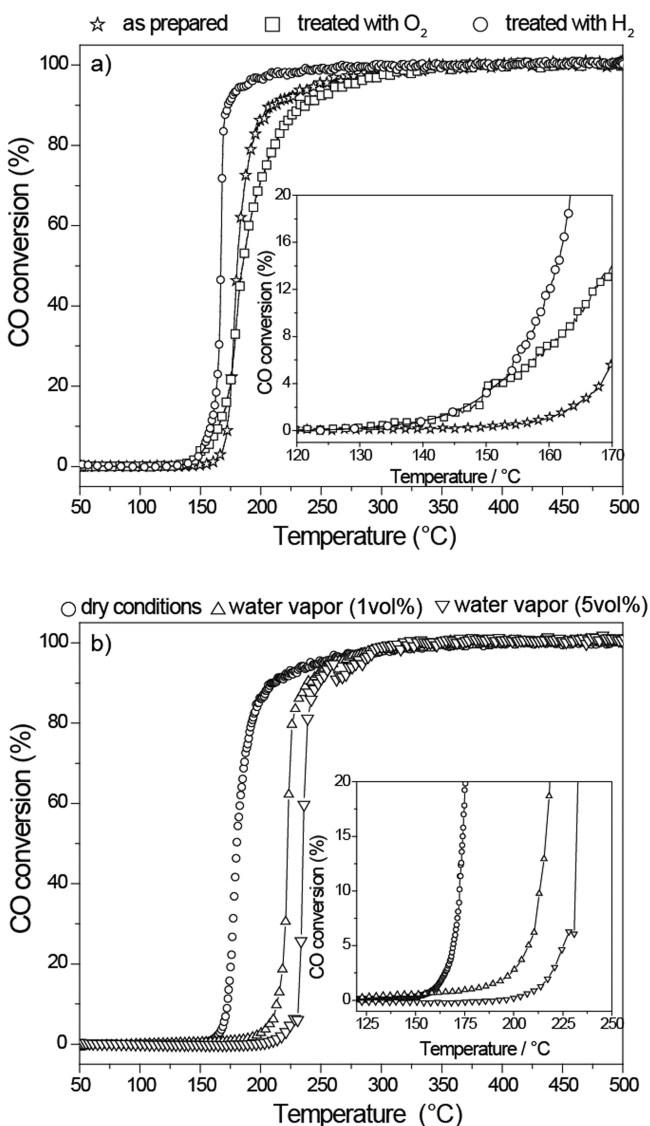


**Figure 6.** Catalytic conversion of CO to CO<sub>2</sub> on Cu/SiO<sub>2</sub> as a function of catalyst pretreatment (a) in dry conditions and (b) in humid conditions (addition of 1 and 5 vol % water vapor).

nanopowder is an inert support and does not participate in the catalytic reaction.<sup>27</sup> The CO oxidation reaction was performed without and with pretreatment of the samples using different atmospheres ( $\text{H}_2$  or  $\text{O}_2$ ) in order to investigate the influence that the species present in the catalyst surface had on the catalytic activity. Wan et al. found that thermal treatment before a catalytic test could promote the activity of Cu catalysts. The

**Table 2.** CO Oxidation Activity of the Cu/SiO<sub>2</sub> Catalysts

pretreatment Cu/SiO <sub>2</sub>	$T_{\text{start}}^a$ (°C)	$T_{50\%}^b$ (°C)	$T_{100\%}^c$ (°C)	rate <sup>d</sup>
as-prepared	135	180	345	4.04
H <sub>2</sub> pretreatment	110	167	240	4.34
O <sub>2</sub> pretreatment	116	185	356	3.78
as-prepared (1 vol % water vapor)	170	220	360	3.28
as-prepared (5 vol % water vapor)	175	235	357	0.23

<sup>a</sup>Temperature of initial conversion. <sup>b</sup>Temperature of 50% of CO conversion. <sup>c</sup>Temperature of 100% of CO conversion. <sup>d</sup>Reaction rate at 225 °C expressed in mmol of CO g<sup>-1</sup> s<sup>-1</sup>.

dispersed  $\text{Cu}^+$  species that originated from the incomplete reduction of the dispersed  $\text{Cu}^{2+}$  played a significant role in low-temperature CO oxidation.<sup>28</sup> The as-sputtered Cu NPs samples, without pretreatment, start the CO oxidation at a temperature near 150 °C and exhibit total conversion of CO to CO<sub>2</sub> at temperatures lower than 345 °C, and it was maintained until 500 °C. In the temperature range of 150–215 °C ( $\Delta t = 65$  °C) a rapid increase of activity up to 90% of conversion was observed.

Although the XRD pattern (Figure 3) showed that the as-prepared Cu/SiO<sub>2</sub> NPs had a metallic phase, the surface was partially oxidized. The XAS and XPS techniques showed that the  $\text{Cu}^0$  and  $\text{Cu}^{2+}$  phases are present in the samples. The XANES spectra of the as-prepared Cu NPs (Figure 4) revealed that the major component is the  $\text{Cu}^0$  phase (85 and 15%  $\text{Cu}^0$  and  $\text{Cu}^{2+}$ , respectively). To investigate the influence of the surface composition on the catalytic activity, we pretreated the sample using different atmospheres ( $\text{H}_2$  to reduce  $\text{Cu}^{2+}$  to  $\text{Cu}^0$  and  $\text{O}_2$  to oxidize  $\text{Cu}^0$  to  $\text{Cu}^{2+}$ ). The activity of the samples subjected to  $\text{H}_2$  pretreatment at 200 °C for 2 h (soft pretreatment) before the CO oxidation reaction was improved (Figure 6).

The temperature at the beginning of the CO oxidation reaction decreased from 150 to 110 °C ( $\Delta t = 40$  °C), as compared with the as-prepared sample. The temperature of total conversion (100%) decreased from 345 to 240 °C ( $\Delta t = 105$  °C). The XANES spectra showed that the pretreated sample at soft conditions (200 °C for 2 h in  $\text{H}_2$ ) increases the  $\text{Cu}^0$  concentration from 85 to 96%. The sample subjected to  $\text{O}_2$  pretreatment at 200 °C for 2 h, showed a lower catalytic activity than the as-prepared sample (without treatment) or the sample with the pretreatment of  $\text{H}_2$  at 200 °C. The goal of treating the Cu/SiO<sub>2</sub> NPs with oxygen was to investigate the catalytic activity of the  $\text{Cu}^{2+}$  phase, because the literature suggests that  $\text{Cu}^{2+}$  is active for CO oxidation.<sup>6</sup> The XANES spectra showed that the pretreated sample at soft conditions (200 °C for 2 h in  $\text{O}_2$ ) increases the  $\text{Cu}^{2+}$  concentration from 15% to 67%. The catalyst previously treated with  $\text{O}_2$  starts to convert CO at 116 °C; it reached 100% of CO conversion at 356 °C and that was maintained until 500 °C. These results clearly indicate that the increase of the  $\text{Cu}^{2+}$  phase decreased the activity of the catalyst. Moreover, both of the catalysts with a higher concentration of the  $\text{Cu}^0$  phase (the as-prepared and  $\text{H}_2$  pretreated samples) exhibited higher activity for the CO oxidation reaction. The  $T_{50}$  value (light-off temperature) for the CO oxidation reaction is quite low for the as-prepared sample and it was slightly lower for the sample pretreated with  $\text{H}_2$  (Table 2).

The reaction rates of the catalysts, expressed by mass of the Cu and calculated at 99% (at 225 °C) of conversion, are shown

in Table 2. The specific rate of the reduced catalyst ( $4.34 \text{ mmol CO s}^{-1} \text{ g}_{\text{Cu}}^{-1}$ ) is higher than those observed in the literature for standard Cu materials and it is comparable to some Pt catalysts.<sup>18,29</sup>

Figure 6b showed the CO oxidation results for Cu/SiO<sub>2</sub> as-prepared catalyst in dry conditions and with the addition of 1 and 5 vol % of water vapor in the feed. The addition of water vapor resulted in an increase of the  $T_{\text{start}}$  from 150 to 170 and 175 °C,  $T_{50\%}$  from 180 to 222 and 235 °C, and  $T_{100\%}$  from 345 to 360 and 357 °C, respectively, for 1 and 5 vol % water vapor. These changes in the reaction temperature can be attributed to the adsorption of water on the catalyst surface, as reported by Debeila et al.<sup>30</sup> for Au-TiO<sub>2</sub> catalyst. In the presence of water vapor, the catalyst exhibited lower reaction rates at 225 °C (Table 2), but it was still able to achieve 100% conversion of CO to CO<sub>2</sub> at higher temperatures. All reactions exhaust gases were monitored by FTIR and in all cases total CO conversion was observed. The bands attributed to CO<sub>2</sub> at 2360 and 2340  $\text{cm}^{-1}$  increased with the temperature (see the Supporting Information, Figures S3 and S4).

The temporal stability is a very important parameter for real application of catalysts in exhausts gases emissions control. Here, stability tests of the Cu NPs catalyst was performed at 350 °C with 100% conversion in dry and humid conditions (Figure 7).

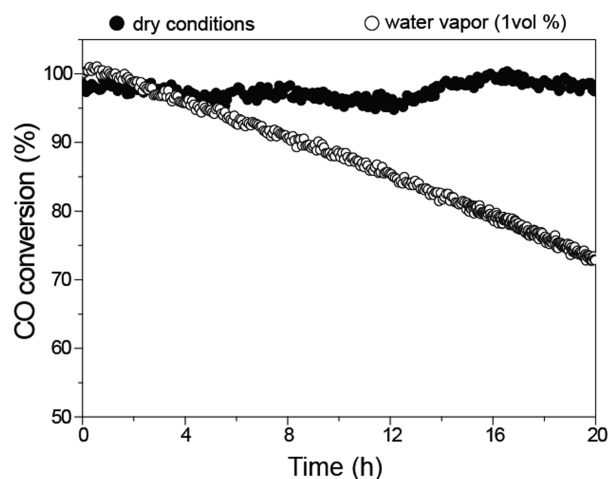


**Figure 7.** Temporal stability of the Cu/SiO<sub>2</sub> on the CO oxidation reaction versus time-on-stream at 350 °C in dry and in humid conditions (addition of 1 vol % of water vapor).

In the stability test performed in dry conditions, the catalyst maintained nearly the same activity for up to 45 h (the first 20 h are shown in Figure 7). However, a significant loss of activity was observed in the stability test in humid conditions (addition of 1 vol % of water vapor). The conversion of CO to CO<sub>2</sub> decreased to ca. 70% after 20 h of time on stream. These results confirmed the high activity and stability of the catalyst for the CO oxidation reaction in dry conditions, but the deactivation process observed in humid conditions still needs to be studied in more detail. The deactivated catalyst was able to partially recover its activity when submitted to dry conditions, eventually approaching the same conversion value as the used catalyst after 20 h.

## CONCLUSION

Metallic Cu NPs with an 8 nm diameter have been successfully prepared on a SiO<sub>2</sub> nanopowder surface by the magnetron sputtering deposition method. Even though Cu<sup>0</sup> was the only phase identified by XRD, the XANES and XPS studies confirmed the partial oxidation of the as-prepared nanoparticles after air exposure. The as-prepared material (85% Cu<sup>0</sup> and 15% Cu<sup>2+</sup>) reveals outstanding catalytic activity for CO oxidation. The sample enriched in the Cu<sup>0</sup> phase by H<sub>2</sub> soft pretreatment (96% Cu<sup>0</sup> and 4% Cu<sup>2+</sup>) similarly exhibited a very good catalytic performance, but the samples previously oxidized with O<sub>2</sub> exhibited a poorer performance when compared to the other two samples. Higher activity and stability were observed for the as-prepared and the H<sub>2</sub> soft pretreatment Cu/SiO<sub>2</sub> samples suggesting that the presence of the Cu<sup>0</sup> species is more important for the formation of the active sites for CO oxidation than other oxide phases (Cu<sup>2+</sup> and Cu<sup>1+</sup>). The presence of humidity caused only a small increase in the temperature require for the reaction to reach 100% conversion, but did affect the stability of the catalyst over time on stream. Therefore, Cu NPs prepared using magnetron sputtering deposition on silica have a high potential for application as a catalyst material for CO oxidation in exhaust gas streams.

## ASSOCIATED CONTENT

### Supporting Information

Details of the SEM images of the SiO<sub>2</sub> nanospheres prepared by the Stöber method, complementary XPS data, and FT-IR analysis. This material is available free of charge via the Internet at <http://pubs.acs.org>.

## AUTHOR INFORMATION

### Corresponding Authors

\*E-mail: [rgoncalves@ifsc.usp.br](mailto:rgoncalves@ifsc.usp.br).

\*E-mail: [lrossi@iq.usp.br](mailto:lrossi@iq.usp.br).

### Present Address

‡R.V.G. is currently at Instituto de Física de São Carlos, Universidade de São Paulo, CP 369, São Carlos 13560-970, SP, Brazil.

### Notes

The authors declare no competing financial interest.

## ACKNOWLEDGMENTS

The authors are grateful for the financial support offered by São Paulo Research Foundation – FAPESP (grant 13/21323-2 and 14/15159-8). Our thanks are also extended to the Brazilian Synchrotron Light Laboratory (LNLS) for use of its XAFS1 experimental facilities (proposal XAFS1-15295 and XAFS1-17154) and its experimental facilities (INTERCOVAMEX Sputtering System (FAPESP grant 11/17402-9)); we also wish to thank LNNano for the use of the FESEM microscope (proposals SEM-FEG 13057).

## REFERENCES

- (1) Prasad, R.; Singh, P. A Review on CO Oxidation Over Copper Chromite Catalyst. *Catal. Rev. Sci. Eng.* **2012**, *54*, 224–279.
- (2) Heo, I.; Yoon, D. Y.; Cho, B. K.; Nam, I.-S.; Choung, J. W.; Yoo, S. Activity and thermal stability of Rh-based catalytic system for an advanced modern TWC. *Appl. Catal. B: Environ.* **2012**, *121–122*, 75–87.

- (3) Kašpar, J.; Fornasiero, P.; Hickey, N. Automotive Catalytic Converters: Current Status and Some Perspectives. *Catal. Today* **2003**, *77*, 419–449.
- (4) Royer, S.; Duprez, D. Catalytic Oxidation of Carbon Monoxide over Transition Metal Oxides. *ChemCatChem* **2011**, *3*, 24–65.
- (5) Goncalves, R. V.; Wojcieszak, R.; Uberman, P. M.; Teixeira, S. R.; Rossi, L. M. Insights Into the Active Surface Species Formed on Ta<sub>2</sub>O<sub>5</sub> Nanotubes in the Catalytic Oxidation of CO. *Phys. Chem. Chem. Phys.* **2014**, *16*, 5755–5762.
- (6) Pillai, U. R.; Deevi, S. Room Temperature Oxidation of Carbon Monoxide Over Copper Oxide Catalyst. *Appl. Catal. B: Environ.* **2006**, *64*, 146–151.
- (7) Huang, T.-J.; Tsai, D.-H. CO Oxidation Behavior of Copper and Copper Oxides. *Catal. Lett.* **2003**, *87*, 173–178.
- (8) Jernigan, G. G.; Somorjai, G. A. Carbon Monoxide Oxidation over Three Different Oxidation States of Copper: Metallic Copper, Copper(I) Oxide, and Copper(II) Oxide - A Surface Science and Kinetic Study. *J. Catal.* **1994**, *147*, 567–577.
- (9) Svintitskiy, D. A.; Chupakhin, A. P.; Slavinskaya, E. M.; Stonkus, O. A.; Stadnichenko, A. I.; Koscheev, S. V.; Boronin, A. I. Study of Cupric Oxide Nanopowders as Efficient Catalysts for Low-temperature CO Oxidation. *J. Mol. Catal. A: Chem.* **2013**, *368–369*, 95–106.
- (10) White, B.; Yin, M.; Hall, A.; Le, D.; Stolbov, S.; Rahman, T.; Turro, N.; O'Brien, S. Complete CO Oxidation over Cu<sub>2</sub>O Nanoparticles Supported on Silica Gel. *Nano Lett.* **2006**, *6*, 2095–2098.
- (11) Wu, G.; Guan, N.; Li, L. Low temperature CO oxidation on Cu<sub>2</sub>O/TiO<sub>2</sub> Catalyst Prepared by Photodeposition. *Catal. Sci. Tech* **2011**, *1*, 601–608.
- (12) Huang, J.; Wang, S.; Zhao, Y.; Wang, X.; Wang, S.; Wu, S.; Zhang, S.; Huang, W. Synthesis and Characterization of CuO/TiO<sub>2</sub> Catalysts for Low-temperature CO Oxidation. *Catal. Commun.* **2006**, *7*, 1029–1034.
- (13) Wang, W.-W.; Du, P.-P.; Zou, S.-H.; He, H.-Y.; Wang, R.-X.; Jin, Z.; Shi, S.; Huang, Y.-Y.; Si, R.; Song, Q.-S.; Jia, C.-J.; Yan, C.-H. Highly Dispersed Copper Oxide Clusters as Active Species in Copper-Ceria Catalyst for Preferential Oxidation of Carbon Monoxide. *ACS Catal.* **2015**, *2088–2099*.
- (14) Wender, H.; Migowski, P.; Feil, A. F.; Teixeira, S. R.; Dupont, J. Sputtering Deposition of Nanoparticles onto Liquid Substrates: Recent Advances and Future Trends. *Coord. Chem. Rev.* **2013**, *257*, 2468–2483.
- (15) Wender, H.; Goncalves, R. V.; Feil, A. F.; Migowski, P.; Poletto, F. S.; Pohlmann, A. R.; Dupont, J.; Teixeira, S. R. Sputtering onto Liquids: From Thin Films to Nanoparticles. *J. Phys. Chem. C* **2011**, *115*, 16362–16367.
- (16) Wender, H.; de Oliveira, L. F.; Migowski, P.; Feil, A. F.; Lissner, E.; Precht, M. H. G.; Teixeira, S. R.; Dupont, J. Ionic Liquid Surface Composition Controls the Size of Gold Nanoparticles Prepared by Sputtering Deposition. *J. Phys. Chem. C* **2010**, *114*, 11764–11768.
- (17) Wender, H.; Migowski, P.; Feil, A. F.; de Oliveira, L. F.; Precht, M. H. G.; Leal, R.; Machado, G.; Teixeira, S. R.; Dupont, J. On the Formation of Anisotropic Gold Nanoparticles by Sputtering onto a Nitrile Functionalised Ionic Liquid. *Phys. Chem. Chem. Phys.* **2011**, *13*, 13552–13557.
- (18) Goncalves, R. V.; Wojcieszak, R.; Uberman, P. M.; Eberhardt, D.; Teixeira-Neto, E.; Teixeira, S. R.; Rossi, L. M. Catalytic Abatement of CO Over Highly Stable Pt Supported on Ta<sub>2</sub>O<sub>5</sub> Nanotubes. *Catal. Commun.* **2014**, *48*, 50–54.
- (19) Luza, L.; Gual, A.; Eberhardt, D.; Teixeira, S. R.; Chiaro, S. S. X.; Dupont, J. Imprinting Catalytically Active Pd Nanoparticles onto Ionic-Liquid-Modified Al<sub>2</sub>O<sub>3</sub> Supports. *ChemCatChem* **2013**, *5*, 2471–2478.
- (20) Bussamara, R.; Eberhardt, D.; Feil, A. F.; Migowski, P.; Wender, H.; de Moraes, D. P.; Machado, G.; Papaleo, R. M.; Teixeira, S. R.; Dupont, J. Sputtering Deposition of Magnetic Ni Nanoparticles Directly onto an Enzyme Surface: A Novel Method to Obtain a Magnetic Biocatalyst. *Chem. Commun.* **2013**, *49*, 1273–1275.
- (21) Sree Harsha, K. S., Chapter 9 - Nucleation and Growth of Films. In *Principles of Vapor Deposition of Thin Films*, Harsha, K. S. S., Ed. Elsevier: Oxford, 2006, 685–829.
- (22) Wasa, K.; Kitabatake, M.; Adachi, H. *Thin Film Materials Technology: Sputtering of Compound Materials*; William Andrew: Norwich, NY, 2004.
- (23) Rossi, L. M.; Shi, L.; Quina, F. H.; Rosenzweig, Z. Stöber Synthesis of Monodispersed Luminescent Silica Nanoparticles for Bioanalytical Assays. *Langmuir* **2005**, *21*, 4277–4280.
- (24) Rodriguez-Carvajal, J. Recent Advances in Magnetic-Structure Determination by Neutron Powder Diffraction. *Physica B* **1993**, *192*, 55–69.
- (25) Ravel, B.; Newville, M. Athena, Artemis, Hephaestus: Data Analysis for X-ray Absorption Spectroscopy Using IFEFFIT. *J. Synchrotron Rad.* **2005**, *12*, 537–541.
- (26) Dahlang, T.; Sven, T. Electronic and Optical Properties of Cu, CuO and Cu<sub>2</sub>O Studied by Electron Spectroscopy. *J. Phys.: Condens. Matter* **2012**, *24*, 175002.
- (27) Schubert, M. M.; Hackenberg, S.; van Veen, A. C.; Muhler, M.; Plzak, V.; Behm, R. J. CO Oxidation over Supported Gold Catalysts—“Inert” and “Active” Support Materials and Their Role for the Oxygen Supply during Reaction. *J. Catal.* **2001**, *197*, 113–122.
- (28) Wan, H.; Wang, Z.; Zhu, J.; Li, X.; Liu, B.; Gao, F.; Dong, L.; Chen, Y. Influence of CO Pretreatment on the Activities of CuO/γ-Al<sub>2</sub>O<sub>3</sub> catalysts in CO+O<sub>2</sub> reaction. *Appl. Catal. B: Environ.* **2008**, *79*, 254–261.
- (29) Liu, L.; Zhou, F.; Wang, L.; Qi, X.; Shi, F.; Deng, Y. Low-temperature CO Oxidation over Supported Pt, Pd Catalysts: Particular Role of FeO<sub>x</sub> Support for Oxygen Supply During Reactions. *J. Catal.* **2010**, *274*, 1–10.
- (30) Debeila, M. A.; Wells, R. P. K.; Anderson, J. A. Influence of Water and Pretreatment Conditions on CO Oxidation over Au/TiO<sub>2</sub>-In<sub>2</sub>O<sub>3</sub> Catalysts. *J. Catal.* **2006**, *239*, 162–172.